Geometric Property of Off Resonance Error Robust Composite Pulse

Shingo Kukita (toranojoh@phys.kindai.ac.jp)
Kindai University
Haruki Kiya
Kindai University
Yasushi Kondo
Kindai University

Research Article

Keywords: Geometric, Pulse Length Error (PLE), Off Resonance Error (ORE)

Posted Date: November 3rd, 2021

DOI: https://doi.org/10.21203/rs.3.rs-1022466/v1

Geometric property of off resonance error robust composite pulse

Shingo Kukita[1)],* Haruki Kiya[1)], and Yasushi Kondo[1)]

[1)] *Department of Physics, Kindai University, Higashi-Osaka 577-8502, Japan*

(Dated: October 29, 2021)

The precision of quantum operations is affected by unavoidable systematic errors. A composite pulse (CP), which has been well investigated in nuclear magnetic resonance (NMR), is a technique that suppresses the influence of systematic errors by replacing a single operation with a sequence of operations. In NMR, there are two typical systematic errors, Pulse Length Error (PLE) and Off Resonance Error (ORE). Recently, it was found that PLE robust CPs have a clear geometric property. In this study, we show that ORE robust CPs also have a simple geometric property, which is associated with trajectories on the Bloch sphere of the corresponding operations. We discuss the geometric property of ORE robust CPs using two examples.

I. INTRODUCTION

Quantum technologies that utilise quantum states, such as quantum computing [1–3] and metrology [4–6], require precise control of the states. However, the quantum systems that we are attempting to control basically experience unavoidable environmental noise and systematic errors caused by experimental apparatuses. They prevent us from precise control of quantum states.

To suppress the effects of systematic errors, a composite pulse (CP) has been investigated [7–9] particularly in the field of nuclear magnetic resonance (NMR), which can be utilised to implement toy quantum computers [10–12]. In CPs, a single operation is replaced by a sequence of operations, and the error in each operation cancels each other. The effectiveness of CPs has been exhibited in NMR [13], ion traps [14], and superconducting circuits [15]. In NMR, two types of errors, Pulse Length Error (PLE) and Off Resonance Error (ORE), in one-qubit operations have been intensively studied. Many CPs that are robust against PLE, such as BB1[16], SCROFULOUS[17] and SK1 [18], have been found. Meanwhile, only a small number of ORE robust CPs for arbitrary one qubit operations, such as CORPSE [19], have been found so far. Recently, it was revealed that PLE robust CPs have a geometric property associated with geometric quantum gates [20]. Additionally, a geometric meaning of robustness against any type of noise is discussed in Ref. [21]; however, it is associated with the geometry of Lie algebras and abstract. A concrete geometric property of ORE robust CPs has not yet been addressed.

In this study, we investigated a geometric property of ORE robust CPs via geometry on a three-dimensional sphere, called the Bloch sphere, on which a state of a qubit is represented by a point while an operation by a rotation. PLE corresponds to the error of the rotational angle of an operation, and ORE corresponds to the error of the rotation axis. We obtained the relation between the ORE robustness of a CP and the mass centre of its trajectory. Further, we illustrated this property using two ORE robust CPs, CORPSE and another CP, which we have newly invented. For some simple cases, this property will help us to obtain new ORE robust CPs intuitively.

The remainder of this paper is organised as follows. We briefly review basic concepts of CPs in Sec. II. In Sec. III, we explain our result on the geometric property of ORE robust gates. Section IV introduces two ORE robust CPs, CORPSE and our proposed CP, and we examine how the geometric picture of ORE robust CPs works. Section V presents the conclusions and discussions.

II. REVIEW OF COMPOSITE PULSES

A. general framework

The Schrödinger equation with a time-dependent Hamiltonian $H(t)$ is

$$\frac{d}{dt}|\Psi(t)\rangle = -iH(t)|\Psi(t)\rangle. \tag{1}$$

* toranojoh@phys.kindai.ac.jp

The formal solution from $t = 0$ to $t = T$ in the Schrödinger picture is given by

$$|\Psi(T)\rangle = \mathcal{T}\exp\Big(-i\int_0^T dtH(t)\Big)|\Psi(0)\rangle, \tag{2}$$

where we introduce the symbol of the time-ordered product:

$$\mathcal{T}(A(t_1)B(t_2)) = \begin{cases} A(t_1)B(t_2) & t_1 > t_2, \\ B(t_2)A(t_1) & t_2 > t_1. \end{cases} \tag{3}$$

Its extension to cases of multiple operators is trivial. If the Hamiltonian is piecewise constant, the time-ordered exponential can also be rewritten as

$$\mathcal{T}\exp\Big(-i\int_0^T dtH(t)\Big) = \exp\big(-i(t_k - t_{k-1})H_k\big)\exp\big(-i(t_{k-1} - t_{k-2})H_{k-1}\big)\cdots\exp\big(-i(t_1 - t_0)H_1\big), \tag{4}$$

where we set $t_0 = 0$ and $t_k = T$ and the Hamiltonian is

$$H(t) = H_i,\ t_{i-1} \le t < t_i,\ (i = 1 \sim k). \tag{5}$$

The index k is the number of periods in which the Hamiltonian is constant. We refer to an operation during the Hamiltonian is constant as an elementary operation. Then, the index k represents the number of elementary operations.

Let us assume that the Hamiltonian is decomposed into two parts:

$$H(t) = H_0(t) + H_{\rm err}(t). \tag{6}$$

The part $H_0(t)$ represents the ideal Hamiltonian, whose corresponding dynamics $U_0(T,0) := \mathcal{T}\exp(-i\int_0^T dtH_0(t))$ will be implemented herein. We can control this part of the Hamiltonian. Meanwhile, $H_{\rm err}(t)$ describes the effect of undesired systematic errors during the operation. The magnitude of $H_{\rm err}(t)$ is assumed to be sufficiently small for the entire time region. (Mathematically, all the matrix components of $H_{\rm err}(t)$ are small.) Either part $H_0(t)$ or $H_{\rm err}(t)$ can have (piecewise) time dependence. We define the state in the interaction picture with respect to $H_0(t)$ as

$$|\Psi_I(t)\rangle := \Big(\mathcal{T}\exp\Big(-i\int_0^t dt' H_0(t')\Big)\Big)^\dagger|\Psi(t)\rangle = U_0^\dagger(t,0)|\Psi(t)\rangle, \tag{7}$$

where $|\Psi(t)\rangle$ is a solution to the Schrödinger equation (1). The state $|\Psi_I(t)\rangle$ satisfies the following equation:

$$\frac{d}{dt}|\Psi_I(t)\rangle = -i\tilde{H}_{\rm err}(t)|\Psi_I(t)\rangle, \tag{8}$$

where $\tilde{H}_{\rm err}(t) := U_0^\dagger(t,0)H_{\rm err}(t)U_0(t,0)$. A formal solution of Eq. (8) is

$$|\Psi_I(T)\rangle = \tilde{U}_{\rm err}(T,0)|\Psi_I(0)\rangle := \mathcal{T}\exp\Big(-i\int_0^T dt\tilde{H}_{\rm err}(t)\Big)|\Psi_I(0)\rangle. \tag{9}$$

By comparing the above equation (9) and the definition of the interaction picture (7), the solution of the Schrödinger equation with the Hamiltonian (6) is written as

$$|\Psi(T)\rangle = U_0(T,0)|\Psi_I(T)\rangle = U_0(T,0)\tilde{U}_{\rm err}(T,0)|\Psi(0)\rangle. \tag{10}$$

We intend to implement the ideal unitary operation $U_0(T,0)$ as accurately as possible under the effect of the error term $H_{\rm err}$. As the magnitude of $H_{\rm err}$ is assumed to be small enough, we can ignore its higher-order terms in $\tilde{U}_{\rm err}(T,0)$, and then

$$\tilde{U}_{\rm err}(T,0) \sim \Big(1 - i\int_0^T dt\tilde{H}_{\rm err}(t)\Big). \tag{11}$$

When the condition

$$\int_0^T dt\tilde{H}_{\rm err}(t) = 0. \tag{12}$$

is satisfied, the operation (10) equals the ideal operation $U_0(T,0)$ for any initial state $|\Psi(0)\rangle$ up to the first order with respect to $\tilde{H}_{\rm err}(t)$. Note that to implement a unitary evolution U as the target operation, there are many choices of $H_0(t)$ that satisfy $U = U_0(T,0)$. If we know the error model $H_{\rm err}(t)$, we can take $H_0(t)$ to satisfy $U = U_0(T,0)$ and Eq. (12) using the degrees of freedom of this choice of $H_0(t)$. Thus, the operation caused by such a Hamiltonian $H_0(t)$ traces the unitary operation U in a robust manner against the specific error model $H_{\rm err}(t)$. Compensating the effect of specific error models by a series of operations is called a CP.

B. Qubit control

The most fundamental quantum system is a two-level system, called a qubit. Hereinafter, we focus on the control of one qubit. The control Hamiltonian of a qubit is given as

$$H_0(t) = \omega(t)\vec{n}(t)\cdot\frac{\vec{\sigma}}{2} := \omega(t)(n_x(t)\frac{\sigma_x}{2} + n_y(t)\frac{\sigma_y}{2} + n_z(t)\frac{\sigma_z}{2}), \tag{13}$$

where the vector $\vec{n}(t) = (n_x, n_y, n_z)$ is a time-dependent unit vector, and $\vec{\sigma} := (\sigma_x, \sigma_y, \sigma_z)$ are the Pauli matrices:

$$\sigma_x = \begin{pmatrix} 0 & 1 \\ 1 & 0 \end{pmatrix},\ \sigma_y = \begin{pmatrix} 0 & -i \\ i & 0 \end{pmatrix},\ \sigma_z = \begin{pmatrix} 1 & 0 \\ 0 & -1 \end{pmatrix}. \tag{14}$$

We implement an arbitrary control of a qubit by adjusting $\omega(t)$ and $\vec{n}(t)$. The time dependence of these controllable parameters is often piecewise constant, as shown in Eq. (5), which corresponds to a sequence of pulses. Note that any state of a qubit can be mapped to a point on a sphere (called the Bloch sphere). In this representation, we map the eigenvectors of σ_z, $|\uparrow\rangle := (1,0)^t$ and $|\downarrow\rangle := (0,1)^t$ to the north pole $\vec{z} = (0,0,1)^t$ and the south pole $-\vec{z} = (0,0,-1)^t$ on the Bloch sphere, respectively. Accordingly, the operation of the qubit by the Hamiltonian (13) with constant ω and $\vec{n}$ corresponds to the rotation with the rotation angle $\theta := \omega\tau$ and the axis $\vec{n}$, where τ is a period during which ω and $\vec{n}$ are applied. Hereinafter, we consider the case where the Hamiltonian is piecewise constant.

When we consider the control of one qubit, there are two types of systematic errors: PLE and ORE.

1. PLE case

PLE is described by the change in $\omega(t)$ in the control Hamiltonian, $\omega(t) \to \omega(t)(1+\epsilon)$, where ϵ is a small parameter representing the magnitude of PLE. The control Hamiltonian $H_0(t)$ and the error Hamiltonian $H_{\rm err}(t)$ are given by

$$H_0(t) = \omega_i\vec{n}_i\cdot\vec{\sigma}/2, \quad H_{\rm err}(t) = \epsilon\omega_i\vec{n}_i\cdot\vec{\sigma}/2, \quad t_{i-1} < t < t_i. \tag{15}$$

Here, we assume that ϵ is constant at $0 < t < T$ because it represents a systematic error. The condition of error robustness (12) in this case is

$$\begin{aligned}
\int_0^T dt\tilde{H}_{\rm err}(t) =& \epsilon\int_0^{t_1} dt e^{i\omega_1 t\vec{n}_1\cdot\vec{\sigma}/2}(\omega_1\vec{n}_1\cdot\vec{\sigma}/2)e^{-i\omega_1 t\vec{n}_1\cdot\vec{\sigma}/2} \\
&+ \epsilon\int_{t_1}^{t_2} dt e^{i\omega_1 t_1\vec{n}_1\cdot\vec{\sigma}/2}e^{i\omega_2(t-t_1)\vec{n}_2\cdot\vec{\sigma}/2}(\omega_2\vec{n}_2\cdot\vec{\sigma}/2)e^{-i\omega_2(t-t_1)\vec{n}_2\cdot\vec{\sigma}/2}e^{-i\omega_1 t_1\vec{n}_1\cdot\vec{\sigma}/2} + \cdots \\
&+ \epsilon\int_{t_{k-1}}^{T} dt e^{i\omega_1 t_1\vec{n}_1\cdot\vec{\sigma}/2}\cdots e^{i\omega_k(t-t_{k-1})\vec{n}_k\cdot\vec{\sigma}/2}(\omega_k\vec{n}_k\cdot\vec{\sigma}/2)e^{-i\omega_k(t-t_{k-1})\vec{n}_k\cdot\vec{\sigma}/2}\cdots e^{-i\omega_1 t_1\vec{n}_1\cdot\vec{\sigma}/2} \\
=& \epsilon\omega_1 t_1(\vec{n}_1\cdot\vec{\sigma}/2) + \epsilon\omega_2(t_2-t_1)e^{i\omega_1 t_1\vec{n}_1\cdot\vec{\sigma}/2}(\vec{n}_2\cdot\vec{\sigma}/2)e^{-i\omega_1 t_1\vec{n}_1\cdot\vec{\sigma}/2} + \cdots \\
&+ \epsilon\omega_k(T-t_{k-1})e^{i\omega_1 t_1\vec{n}_1\cdot\vec{\sigma}/2}\cdots e^{i\omega_{k-1}(t_{k-1}-t_{k-2})\vec{n}_{k-1}\cdot\vec{\sigma}/2}(\vec{n}_k\cdot\vec{\sigma}/2)e^{-i\omega_1 t_1\vec{n}_1\cdot\vec{\sigma}/2}\cdots e^{i\omega_{k-1}(t_{k-1}-t_{k-2})\vec{n}_{k-1}\cdot\vec{\sigma}/2} \\
=& \epsilon\sum_{i=1}^{k} V_0^\dagger\cdots V_{i-1}^\dagger(\theta_i\vec{n}_i\cdot\vec{\sigma}/2)V_{i-1}\cdot\cdots\cdot V_0 = 0.
\end{aligned} \tag{16}$$

where $\theta_i := \omega_i(t_i - t_{i-1})$, and V_i denotes $\exp(-i\theta_i\vec{n}_i\cdot\vec{\sigma}/2)$ while V_0 is the identity matrix. In Ref [20], it is shown that if the above error robustness condition for PLE is satisfied, the operation by $H_0(t)$ in Eq. (15) is a geometric quantum gate [22–24] based on the concept of holonomy [25–28]. Many PLE robust CPs, such as BB1[16], SCROFULOUS[17], and SK1 [18], have been found to date.

2. ORE case

ORE is typically caused by the miscalibration of the resonance frequency of a qubit. When the quantisation axis is the z-axis of the Bloch sphere, the Hamiltonian with ORE has an error term proportional to σ_z:

$$H(t) = H_0(t) + H_{\rm err}(t) := \omega\vec{n}(t)\cdot\frac{\vec{\sigma}}{2} + f\frac{\sigma_z}{2}, \tag{17}$$

where f is a small parameter corresponding to ORE magnitude. For later convenience, we assume in the above equation that we control the direction $\vec{n}(t)$ and ω is constant during the operation, which is often desirable in NMR. We then take $\omega = 1$ without loss of generality, where t and f are non-dimensional parameters. Note that the error term for ORE is time independent. The condition (12) is calculated as

$$\begin{aligned}\int_0^T dt\tilde{H}_{\rm err}(t) =& f\int_0^{t_1} dt e^{it\vec{n}_1\cdot\vec{\sigma}/2}\frac{\sigma_z}{2}e^{-it\vec{n}_1\cdot\vec{\sigma}/2}\\ &+ f\int_{t_1}^{t_2} dt e^{it_1\vec{n}_1\cdot\vec{\sigma}/2}e^{i(t-t_1)\vec{n}_2\cdot\vec{\sigma}/2}\frac{\sigma_z}{2}e^{-i(t-t_1)\vec{n}_2\cdot\vec{\sigma}/2}e^{-it_1\vec{n}_1\cdot\vec{\sigma}/2}+\cdots\\ &+ f\int_{t_{k-1}}^{T} dt e^{it_1\vec{n}_1\cdot\vec{\sigma}/2}\cdots e^{i(t-t_{k-1})\vec{n}_k\cdot\vec{\sigma}/2}\frac{\sigma_z}{2}e^{-i(t-t_{k-1})\vec{n}_k\cdot\vec{\sigma}/2}\cdots e^{-it_1\vec{n}_1\cdot\vec{\sigma}/2}\\ =& f\sum_{i=1}^{k} V_0^\dagger\cdots V_{i-1}^\dagger\Big(\int_{t_{i-1}}^{t_i} dt e^{i(t-t_{i-1})\vec{n}_1\cdot\vec{\sigma}/2}\frac{\sigma_z}{2}e^{-i(t-t_{i-1})\vec{n}_1\cdot\vec{\sigma}/2}\Big)V_{i-1}\cdots V_0 = 0, \end{aligned} \tag{18}$$

for a piecewise constant Hamiltonian. This ORE robustness condition seems to be more complicated than that of PLE (16). However, in this study, we show that this condition has a simple geometric property via geometry on the Bloch sphere.

CORPSE, which was proposed in Ref. [19], is a well known ORE robust CP. This CP can perform an arbitrary θ rotation in an ORE robust manner with considerably simple operations. Other possibilities of ORE robust CPs, however, have seldom been considered.

III. GEOMETRIC PROPERTY OF ORE ROBUST CP

Here, we explain a geometric property of Eq. (18). First, note that for any 3-dimensional unit vector $\vec{n}$ and $\vec{m}$,

$$e^{-i\theta\vec{m}\cdot\vec{\sigma}/2}(\vec{n}\cdot\vec{\sigma})e^{i\theta\vec{m}\cdot\vec{\sigma}/2} = \big(\boldsymbol{R}(\theta,\vec{m})\vec{n}\big)\cdot\vec{\sigma}, \tag{19}$$

where $\boldsymbol{R}(\theta,\vec{m})$ is a 3×3 rotation matrix with rotational axis $\vec{m}$ and angle θ. Using this equality, the right hand side of Eq. (18) can be rewritten as

$$\begin{aligned} & f\sum_{i=1}^{k} V_0^\dagger\cdots V_{i-1}^\dagger\Big(\int_{t_{i-1}}^{t_i} dt e^{i(t-t_{i-1})\vec{n}_1\cdot\vec{\sigma}/2}\frac{\sigma_z}{2}e^{-i(t-t_{i-1})\vec{n}_1\cdot\vec{\sigma}/2}\Big)V_{i-1}\cdots V_0\\ &= f\sum_{i=1}^{k} V_0^\dagger\cdots V_{i-1}^\dagger\Big(\int_{t_{i-1}}^{t_i} dt e^{i(t-t_{i-1})\vec{n}_1\cdot\vec{\sigma}/2}(\vec{z}\cdot\frac{\vec{\sigma}}{2})e^{-i(t-t_{i-1})\vec{n}_1\cdot\vec{\sigma}/2}\Big)V_{i-1}\cdots V_0\\ &= f\left(\sum_{i=1}^{k}\boldsymbol{R}^{-1}(\theta_1,\vec{n}_1)\boldsymbol{R}^{-1}(\theta_2,\vec{n}_2)\cdots\boldsymbol{R}^{-1}(\theta_{i-1},\vec{n}_{i-1})\int_{t_{i-1}}^{t_i} dt\boldsymbol{R}^{-1}(t-t_{i-1},\vec{n}_i)\vec{z}\right)\cdot\frac{\vec{\sigma}}{2}. \end{aligned} \tag{20}$$

Thus, we obtain the following condition from Eq. (18),

$$\sum_{i=1}^{k}\Big(\boldsymbol{R}^{-1}(\theta_1,\vec{n}_1)\boldsymbol{R}^{-1}(\theta_2,\vec{n}_2)\cdots\boldsymbol{R}^{-1}(\theta_{i-1},\vec{n}_{i-1})\int_{t_{i-1}}^{t_i} dt\boldsymbol{R}^{-1}(t-t_{i-1},\vec{n}_i)\vec{z}\Big) = \vec{0}. \tag{21}$$

This is also equivalent to the condition:

$$\begin{aligned} & \vec{p}^{\,t}\cdot\left(\sum_{i=1}^{k}\Big(\boldsymbol{R}^{-1}(\theta_1,\vec{n}_1)\boldsymbol{R}^{-1}(\theta_2,\vec{n}_2)\cdots\boldsymbol{R}^{-1}(\theta_{i-1},\vec{n}_{i-1})\int_{t_{i-1}}^{t_i} dt\boldsymbol{R}^{-1}(t-t_{i-1},\vec{n}_i)\vec{z}\Big)\right) = 0, \quad \forall\vec{p}\in\mathbb{R}^3\\ \Longleftrightarrow & \vec{z}^{\,t}\cdot\left(\sum_{i=1}^{k}\int_{t_{i-1}}^{t_i} dt\boldsymbol{R}(t-t_{i-1},\vec{n}_i)\vec{p}_{i-1}\right) = 0, \quad \forall\vec{p}\in\mathbb{R}^3, \end{aligned} \tag{22}$$

where $\vec{p}_i := \boldsymbol{R}(\theta_i,\vec{n}_i)\cdots\boldsymbol{R}(\theta_1,\vec{n}_1)\vec{p}$ with $\vec{p}_0 := \vec{p}$. In the second line, we transpose the equation and use $\boldsymbol{R}^t(\theta,\vec{m}) = \boldsymbol{R}^{-1}(\theta,\vec{m})$. As the above equation is linear, we can normalise the length of $\vec{p}$ without loss of generality, and then

we identify $\vec{p}$ with a position vector (quantum state) on the Bloch sphere. Let $\mathbb{R}_n^3$ denote the space of the position vectors on the Bloch sphere.

$\vec{p}_i$ represents the point after the sequence of rotations $\boldsymbol{R}(\theta_i, \vec{n}_i)\boldsymbol{R}(\theta_{i-1}, \vec{n}_{i-1}) \cdots \boldsymbol{R}(\theta_1, \vec{n}_1)$. By introducing $\vec{p}(t) := \boldsymbol{R}(t - t_{i-1}, \vec{n}_i)p_{i-1}$ $(t_{i-1} \leq t < t_i)$, we further summarise Eq. (22) as

$$\vec{z}^{\,t} \cdot \int_0^T dt\vec{p}(t) = 0, \quad \forall \vec{p} \in \mathbb{R}_n^3. \tag{23}$$

The integration in the above equation is the sum of all position vectors on the trajectory,

$$\vec{p}(t): \ \vec{p} \xrightarrow{\boldsymbol{R}(\theta_1,\vec{n}_1)} \vec{p}_1 \xrightarrow{\boldsymbol{R}(\theta_2,\vec{n}_2)} \cdots \xrightarrow{\boldsymbol{R}(\theta_k,\vec{n}_k)} \vec{p}_k. \tag{24}$$

See Fig. 1. This sequence of rotations corresponds to the action of the errorless unitary operation $V_k \cdots V_1$ in the Bloch sphere representation.

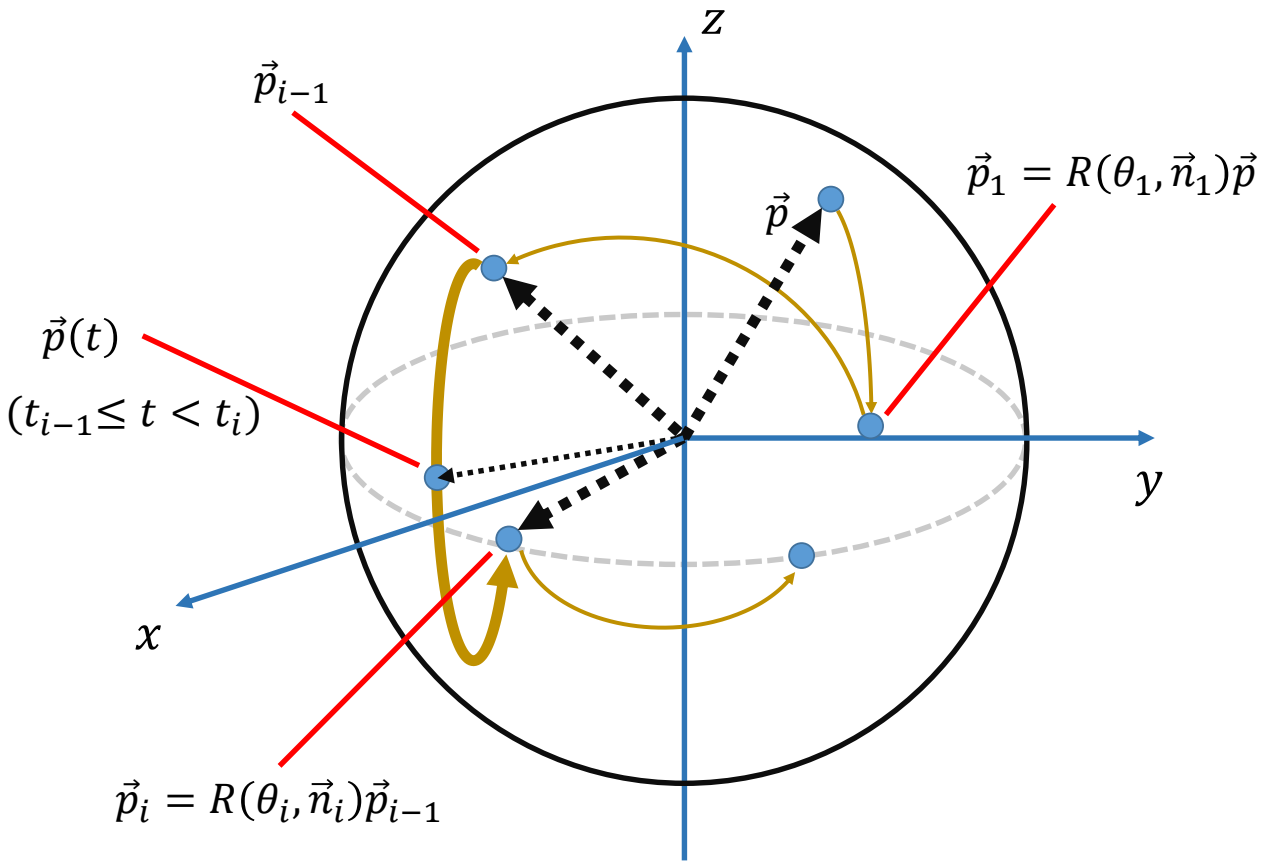

FIG. 1. Schematic picture of the trajectory of $\vec{p}$ by $\boldsymbol{R}(\theta_k, \vec{n}_k) \cdots \boldsymbol{R}(\theta_1, \vec{n}_1)$ on the Bloch sphere. The thick curve represents the trajectory of the i-th operation from $\vec{p}_{i-1}$ to $\vec{p}_i$. The i-th part of the summation in Eq. (22) is the integration of all position vectors along this trajectory.

From the viewpoint of geometry, the sum of all position vectors in Eq. (23) has a clear meaning as (the total mass) $\times$ (the mass centre of the trajectory) when we assign a constant line density of "mass" on the trajectory. Because the total mass gives just a non-zero constant factor, the condition (22) is equivalent to the following simple equation:

$$\vec{z}^{\,t} \cdot \vec{M}_{\vec{p}} = 0, \quad \forall \vec{p} \in \mathbb{R}_n^3, \tag{25}$$

where $\vec{M}_{\vec{p}}$ is the mass centre of the trajectory. This immediately implies that *the mass centre of the errorless trajectory by a CP on the Bloch sphere exists on the xy plane for any initial state if and only if this CP is ORE robust.* This is the geometric property of ORE robust CPs. Note that this geometric property is also valid when the Hamiltonian is not piecewise constant but continuously time-dependent.

IV. TWO EXAMPLES OF ORE ROBUST COMPOSITE PULSES

In this section, we verify that the mass centre of the trajectory lies on the xy plane for two ORE robust CPs: CORPSE and our proposed CP. First, we explain the notation. In a basic NMR setup, the unit vector $\vec{n}$ for each operation $e^{-i\theta\vec{n}\cdot\vec{\sigma}/2}$ is directed into the xy plane. Without loss of generality, we can represent $\vec{n}$ by $\vec{n}_\phi := (\cos\phi, \sin\phi, 0)$. We parametrise an operation by θ and ϕ, and thus define $(\theta)_\phi := e^{-i\theta\vec{n}_\phi\cdot\vec{\sigma}/2}$. Accordingly, a CP is written as a sequence $(\theta_k)_{\phi_k}(\theta_{k-1})_{\phi_{k-1}}\cdots(\theta_1)_{\phi_1}$.

A. CORPSE

A well-known ORE robust CP, CORPSE, can implement $(\theta)_\phi$ as the target operation for any θ and ϕ. The CORPSE sequence of implementing $(\theta)_\phi$ comprises three elementary operations ($k = 3$) given by the following parameters:

$$\theta_1 = 2n_1\pi + \theta/2 - \kappa,\ \theta_2 = 2n_2\pi - 2\kappa,\ \theta_3 = 2n_3\pi + \theta/2 - \kappa,\quad \phi_1 = \phi_2 - \pi = \phi_3 = \phi, \tag{26}$$

where $\kappa = \arcsin(\sin(\theta/2)/2)$ and n_i $(i = 1, 2, 3)$ are integers that satisfy $n_1, n_3 \geq 0$, and $n_2 \geq 1$. Simple algebraic calculations show that the CORPSE sequence $(\theta_3)_{\phi_3}(\theta_2)_{\phi_2}(\theta_1)_{\phi_1}$ satisfies $(\theta)_\phi = (\theta_3)_{\phi_3}(\theta_2)_{\phi_2}(\theta_1)_{\phi_1}$ and is ORE robust.

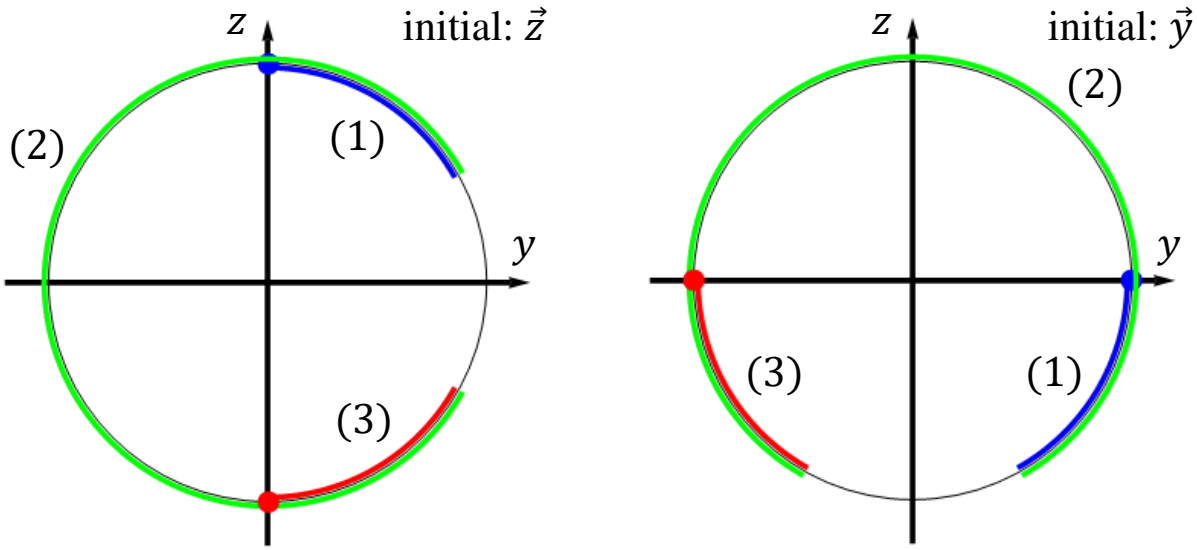

FIG. 2. Errorless trajectories by CORPSE on the yz plane. The left (right) panel has $\vec{z}$ ($\vec{y}$) as the initial state. The initial (final) states are represented by the blue (red) points. The blue, green, and red curves represent the first, second, and third pulse trajectories, respectively. The left (right) panel has $\vec{z}$ ($\vec{y}$) as the initial state.

We show the ORE robustness of CORPSE from a geometric viewpoint. For simplicity, we consider the case in which CORPSE implement $(\pi)_0$, that is, the π rotation in the direction $\vec{x} := (1, 0, 0)$. Also, we take $n_1 = n_3 = 0$ and $n_2 = 1$. The parameters for this case are $\theta_1 = \theta_3 = \pi/3$, $\theta_2 = 5\pi/3$, $\phi_1 = \phi_3 = 0$, and $\phi_2 = \pi$. First, we note that it is only necessary to consider three linear independent unit vectors as $\vec{p}$ to examine the condition (25) owing to the linearity. We take $\vec{x} = (1, 0, 0)^t$, $\vec{y} = (0, 1, 0)^t$, $\vec{z} = (0, 0, 1)^t$ as $\vec{p}$. The vector $\vec{x}$ is a fixed point during the entire operation, and thus, the mass centre of the trajectory starting from $\vec{x}$ is also on that plane. We then examine the trajectory from $\vec{y}$ and $\vec{z}$. It is convenient to show the yz plane to consider the mass centre of the trajectory from $\vec{y}$

and $\vec{z}$ (Fig. 2). The mass centre of the trajectory from $\vec{z}$ is calculated as follows.

$$\begin{aligned}\int_0^T dt\vec{p}(t) &= \int_0^{\frac{\pi}{3}} d\theta \boldsymbol{R}(\theta,\vec{x})(0,0,1)^t + \int_0^{\frac{5\pi}{3}} d\theta \boldsymbol{R}(\theta,-\vec{x})\Big(0,\sin(\frac{\pi}{3}),\cos(\frac{\pi}{3})\Big)^t + \int_0^{\frac{\pi}{3}} d\theta \boldsymbol{R}(\theta,\vec{x})\Big(0,\sin(\frac{2\pi}{3}),\cos(\frac{2\pi}{3})\Big)^t \\ &= \left(\int_0^{\frac{\pi}{3}} - \int_{\frac{\pi}{3}}^{\frac{2\pi}{3}} + \int_{\frac{2\pi}{3}}^{\pi}\right) d\theta(0,\sin\theta,\cos\theta)^t \\ &= [(0,-\cos\theta,\sin\theta)^t]_0^{\frac{\pi}{3}} - [(0,-\cos\theta,\sin\theta)^t]_{\frac{\pi}{3}}^{\frac{2\pi}{3}} + [(0,-\cos\theta,\sin\theta)^t]_{\frac{2\pi}{3}}^{\pi} = \vec{0}. \end{aligned} \tag{27}$$

Accordingly $\vec{M}_{\vec{z}} = \vec{0}$ and thus $\vec{z}^{\,t} \cdot \vec{M}_{\vec{z}} = \vec{z}^{\,t} \cdot \vec{0} = 0$. It is also shown that $\vec{M}_{\vec{y}} = \vec{0}$ because the trajectories from $\vec{y}$ and $\vec{z}$ (and these mass centres) are related by $\frac{\pi}{2}$-rotation. Refer to Fig. 2. Thus, the condition (25) is satisfied for CORPSE.

B. CORP^{2}SE (Compensation for Off Resonance with a Perpendicularly combined Pulse SEquence)

CORPSE is a $k = 3$ symmetric CP satisfying $\phi_1 + \pi = \phi_2$ ($\vec{n}_1 \cdot \vec{n}_2 = -1$). It is a natural question whether there exists a symmetric $k = 3$ CP with the condition $\phi_1 + \pi/2 = \phi_2$ ($\vec{n}_1 \cdot \vec{n}_2 = 0$). Under the assumption that $\vec{n}_1 \cdot \vec{n}_2 = 0$, we find the following symmetric $k = 3$ CP that implements $(\theta)_\phi$:

$$\begin{aligned} &\theta_1 = \theta_3 = \arcsin\Big(-\sqrt{\frac{1-\alpha^2}{1+\alpha^2}}\Big), \quad \theta_2 = \arccos(\alpha^2) \\ &\phi_1 + \pi/4 = \phi_3 + \pi/4 = \phi_2 - \pi/4 = \phi, \end{aligned} \tag{28}$$

where $\alpha = \cos(\theta/2)$. We named this sequence CORP^{2}SE (*Compensation for Off Resonance with a Perpendicularly constructed Pulse SEquence*). CORPSE has the same rotation axis for all elementary operations whereas CORP^{2}SE has one orthogonal rotation axis at the middle operation. In Materials, we evaluate the performance of CORP^{2}SE comparing with CORPSE.

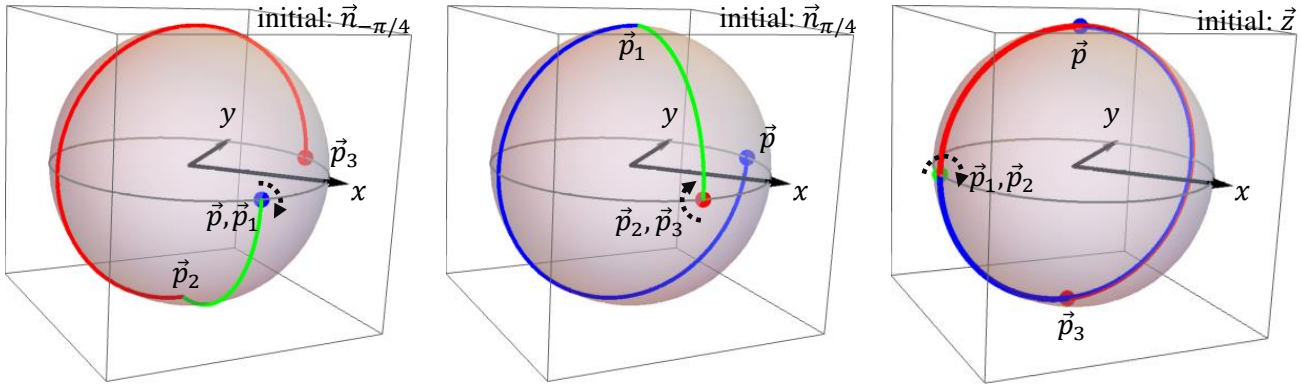

FIG. 3. Errorless trajectories by CORP^{2}SE. The left, middle, and right panels show $\vec{n}_{-\pi/4}$, $\vec{n}_{\pi/4}$, and $\vec{z}$ as the initial state. The initial (final) states are represented by the blue (red) points. The blue, green, and red lines represent the first, second, and third pulse trajectories, respectively. The black arrows show the action of pulses when the state remains at a fixed point of the pulse.

We consider the case in which CORP^{2}SE (28) performs $(\pi)_0$. The parameters are taken to be $\theta_1 = \theta_3 = \frac{3\pi}{2}$, $\theta_2 = \pi/2$, and $\phi_1 = \phi_3 = -\phi_2 = -\frac{\pi}{4}$. In Fig. 3, we show the errorless trajectories from $\vec{z}$, $\vec{n}_{-\pi/4} = \frac{1}{\sqrt{2}}(1,-1,0)$, and $\vec{n}_{\pi/4} = \frac{1}{\sqrt{2}}(1,1,0)$, which are convenient to evaluate the mass centres of trajectories. Each trajectory has the same length on the northern and southern hemispheres. For instance, the trajectory from $\vec{z}$ (right panel) has a length of $3 \times \pi/2$ for each hemisphere. In general, it is not sufficient to consider only the length of arcs for evaluating the mass centre. However, the mass centre of each $\pi/2$ arc in these trajectories has the same absolute value of the z-component. This implies that simply counting the number of $\pi/2$ arcs on each hemisphere is sufficient to evaluate the mass centres in this case. Thus, for π-rotation, we graphically confirm that this CORP^{2}SE is ORE robust.

V. CONCLUSIONS AND DISCUSSIONS

In this study, we found the geometric property of the ORE robustness condition. For any ORE robust CP, its errorless trajectory from any point on the Bloch sphere has its mass centre on the xy plane. The converse of this statement is also true. Moreover, we found that there are many possibilities for ORE robust CPs other than CORPSE even when we use only three elementary operations $k = 3$. For CORPSE and our proposed ORE robust CP, CORP^{2}SE, we confirmed that the mass centres of their trajectories from any initial point are on the xy plane on the Bloch sphere, as expected. Until now, only the geometric property of PLE robust pulses has been concretely known, and ORE robust CPs have not been well investigated. One reason for this is that the error term of ORE does not commute with the control Hamiltonian even at the same time unlike PLE. This makes the analysis of the ORE robust condition difficult algebraically. Our results of the geometric property will increase the tractability of ORE robust CPs.

Here, we intend to discuss what happens if the magnitude of the control field ω is not constant throughout the dynamics. Even in this case, the interpretation of the mass centre is still valid, although the mass density of the trajectories is no longer uniform. We should assign a mass density proportional to the time-dependent $1/\omega(t)$ at each point of trajectories. When we consider a time-dependent $\omega(t)$, it will be more complicated to construct an ORE robust CP. Meanwhile, this implies that we can have more degrees of freedom to construction of ORE robust CPs in such a case.

[1] Bennett, C. H. & DiVincenzo, D. P. Quantum information and computation. *nature* **404**, 247–255 (2000).
[2] Nielsen, M. & Chuang, I. *Quantum Computation and Quantum Information*. Cambridge Series on Information and the Natural Sciences (Cambridge University Press, 2000). URL `https://books.google.co.jp/books?id=aai-P4V9GJ8C`.
[3] Nakahara, M. *Quantum computing: from linear algebra to physical realizations* (CRC press, 2008).
[4] Helstrom, C. W. *Quantum detection and estimation theory*, vol. 84 (Academic press New York, 1976).
[5] Caves, C. M. Quantum-mechanical noise in an interferometer. *Physical Review D* **23**, 1693 (1981).
[6] Holevo, A. S. *Probabilistic and statistical aspects of quantum theory*, vol. 1 (Springer Science & Business Media, 2011).
[7] Counsell, C., Levitt, M. & Ernst, R. Analytical theory of composite pulses. *Journal of Magnetic Resonance (1969)* **63**, 133–141 (1985).
[8] Levitt, M. H. Composite pulses. *Progress in Nuclear Magnetic Resonance Spectroscopy* **18**, 61–122 (1986).
[9] Claridge, T. D. *High-resolution NMR techniques in organic chemistry*, vol. 27 (Elsevier, 2016).
[10] Gershenfeld, N. A. & Chuang, I. L. Bulk spin-resonance quantum computation. *science* **275**, 350–356 (1997).
[11] Cory, D. G., Fahmy, A. F. & Havel, T. F. Ensemble quantum computing by nmr spectroscopy. *Proceedings of the National Academy of Sciences* **94**, 1634–1639 (1997).
[12] Vandersypen, L. M. *et al.* Experimental realization of shor's quantum factoring algorithm using nuclear magnetic resonance. *Nature* **414**, 883–887 (2001).
[13] Bando, M. *et al.* Concatenated composite pulses applied to liquid-state nuclear magnetic resonance spectroscopy. *Scientific reports* **10**, 1–10 (2020).
[14] Gulde, S. *et al.* Implementation of the deutsch–jozsa algorithm on an ion-trap quantum computer. *Nature* **421**, 48–50 (2003).
[15] Collin, E. *et al.* Nmr-like control of a quantum bit superconducting circuit. *Physical review letters* **93**, 157005 (2004).
[16] Wimperis, S. Broadband, narrowband, and passband composite pulses for use in advanced nmr experiments. *Journal of Magnetic Resonance, Series A* **109**, 221–231 (1994).
[17] Cummins, H. K., Llewellyn, G. & Jones, J. A. Tackling systematic errors in quantum logic gates with composite rotations. *Physical Review A* **67**, 042308 (2003).
[18] Brown, K. R., Harrow, A. W. & Chuang, I. L. Arbitrarily accurate composite pulse sequences. *Physical Review A* **70**, 052318 (2004).
[19] Cummins, H. & Jones, J. Use of composite rotations to correct systematic errors in nmr quantum computation. *New Journal of Physics* **2**, 6 (2000).
[20] Kondo, Y. & Bando, M. Geometric quantum gates, composite pulses, and trotter–suzuki formulas. *Journal of the Physical Society of Japan* **80**, 054002 (2011).
[21] Merrill, J. T. & Brown, K. R. Progress in compensating pulse sequences for quantum computation. *Quantum Information and Computation for Chemistry* 241–294 (2014).
[22] Zanardi, P. & Rasetti, M. Holonomic quantum computation. *Physics Letters A* **264**, 94–99 (1999).
[23] Zhu, S.-L. & Wang, Z. Implementation of universal quantum gates based on nonadiabatic geometric phases. *Physical review letters* **89**, 097902 (2002).
[24] Ota, Y. & Kondo, Y. Composite pulses in nmr as nonadiabatic geometric quantum gates. *Physical Review A* **80**, 024302 (2009).
[25] Berry, M. V. Quantal phase factors accompanying adiabatic changes. *Proceedings of the Royal Society of London. A.*

Mathematical and Physical Sciences **392**, 45–57 (1984).
[26] Page, D. N. Geometrical description of berry's phase. *Physical Review A* **36**, 3479 (1987).
[27] Aharonov, Y. & Anandan, J. Phase change during a cyclic quantum evolution. *Physical Review Letters* **58**, 1593 (1987).
[28] Nakahara, M. *Geometry, topology and physics* (CRC press, 2018).

ACKNOWLEDGMENT

This work was supported by JSPS Grants-in-Aid for Scientific Research (21K03423) and CREST (JPMJCR1774).

AUTHOR CONTRIBUTIONS

All the authors contributed equally to this work.

Supplementary Files

This is a list of supplementary files associated with this preprint. Click to download.

- materials.pdf